Experimental Neurology 383 (2025) 114991

Contents lists available at ScienceDirect

Experimental Neurology

journal homepage: www.elsevier.com/locate/yexnr

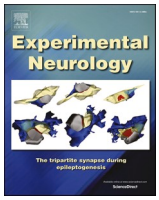

Research paper

Differential impact of optogenetic stimulation of direct and indirect pathways from dorsolateral and dorsomedial striatum on motor symptoms in Huntington's disease mice

Sara Conde-Berriozabal [a,b,c], Laia Sitjà-Roqueta [a,b,c], Esther García-García [a,b,c], Lia García-Gilabert [a,b,c], Anna Sancho-Balsells [a,b,c], Sara Fernández-García [a,b,c], Ened Rodriguez-Urgellés [a,b,c], Albert Giralt [a,b,c], Anna Castañé [a,d], Manuel J. Rodríguez [a,b,c], Jordi Alberch [a,b,c], Mercè Masana [a,b,c,*]

[a] Department of Biomedical Sciences, School of Medicine and Health Sciences, Institute of Neurosciences, Universitat de Barcelona, 08036 Barcelona, Spain
[b] August Pi i Sunyer Biomedical Research Institute (IDIBAPS), 08036 Barcelona, Spain
[c] Centro de Investigación Biomédica en Red sobre Enfermedades Neurodegenerativas (CIBERNED), Instituto de Salud Carlos III, Spain
[d] Universitat de Vic-Universitat Central de Catalunya (UVIC-UCC), Spain

ARTICLE INFO

Keywords:
Optogenetics
Basal ganglia circuits
Locomotion
Motor learning
Movement disorders

ABSTRACT

The alterations in the basal ganglia circuitry are core pathological hallmark in Huntington's Disease (HD) and traditionally linked to its sever motor symptoms. Recently it was shown that optogenetic stimulation of cortical afferences to the striatum is able to reverse motor symptoms in HD mice. However, the specific contribution of the direct and indirect striatal output pathways from the dorsolateral (DLS) and dorsomedial striatum (DMS) to the motor phenotype is still not clear. Here, we aim to uncover the contributions of these striatal subcircuits to motor control in wild type (WT) and HD mice by using the symptomatic R6/1 mice. We systematically evaluated locomotion, exploratory behavior, and motor learning effects of the selective optogenetic stimulation of D1 or A2A expressing neurons (direct and indirect pathway, respectively), in DLS or DMS. Bilateral optogenetic stimulation of the direct pathway from DLS and the indirect pathway from DMS resulted in subtle locomotor enhancements, while unaltering exploratory behavior. Additionally, bilateral stimulation of the indirect pathway from the DLS improved performance in the accelerated rotarod task, suggesting a role in motor learning. In contrast, in HD mice, stimulation of these pathways did not modulate any of these behaviors. Overall, this study highlights that selective stimulation of direct and indirect pathways from DLS and DMS have subtle impact in locomotion, exploratory activity or motor learning. The lack of responses in HD mice also suggests that strategies involving cortico-striatal circuits rather than striatal output circuits might be a better strategy for managing motor symptoms in movement disorders.

1. Introduction

The dysregulation of basal ganglia circuitry stands as the primary cause behind the manifestation of motor abnormalities in Huntington's disease (HD). HD is a progressive neurodegenerative disorder that courses with a triad of motor, cognitive and psychiatric symptoms. It is caused by a polyglutamine expansion in the huntingtin gene (MacDonald et al., 1993), that leads to the degeneration of GABAergic medium-sized spiny neurons (MSNs) of the caudate and putamen nuclei (striatum), the central hub of basal ganglia circuitry.

The medium-sized spiny neurons (MSNs) from the striatum receive inputs from the cortex and thalamus and transmit information through two main pathways, direct and indirect, each projecting to specific output nuclei. Specifically, MSNs from the direct pathway express dopamine D1 receptors and project to the internal globus pallidum (GPi) and the substantia nigra reticulata (SNr); while MSNs from the indirect pathway express dopamine D2 and A2a receptors and project to external globus pallidum (GPe) (Galvan et al., 2012). In addition, the dorsal

* Corresponding author at: Department of Biomedical Sciences, School of Medicine and Health Sciences, Institute of Neurosciences, Universitat de Barcelona, 08036 Barcelona, Spain.
E-mail address: mmasana@ub.edu (M. Masana).

https://doi.org/10.1016/j.expneurol.2024.114991
Received 23 August 2024; Received in revised form 25 September 2024; Accepted 7 October 2024
Available online 9 October 2024

striatum can be further divided by dorsomedial (DMS) and dorsolateral (DLS) regions, based on the clear segregation of cortical inputs along the mediolateral and dorsoventral axes (Hintiryan et al., 2016; Hunnicutt et al., 2016; Wall et al., 2013). For instance, cingulate, orbitofrontal and medial prefrontal cortices project mainly to the DMS, while motor and somatosensorial cortices project preferentially to the DLS (Hintiryan et al., 2016; Hunnicutt et al., 2016). Notably, both direct and indirect pathways project to their specific output nuclei with segregated mediolateral connections (Lee et al., 2020; Lerner et al., 2015). Moreover, activation of direct or indirect pathways has been linked to the induction or inhibition of movement (Durieux et al., 2012; Kravitz et al., 2010), respectively. Yet, it is now accepted that a more complex and coordinated activity of the distinct striatal subcircuits modulates locomotion and motor learning processes (Badreddine et al., 2022; Cui et al., 2013; Kupferschmidt et al., 2017; Tecuapetla et al., 2016; Yin et al., 2009).

However, despite our extensive knowledge of the basal ganglia circuitry under healthy conditions, the involvement of these distinct subcircuits in HD remains limited. In individuals with HD, neurodegeneration primarily occurs in the MSNs of the indirect pathway, with MSNs from the direct pathway being altered later in the course of the disease (Deng et al., 2004; Glass et al., 2000; Reiner et al., 1988; Richfield et al., 1991; Sapp et al., 1995). In mouse models of HD, alterations are observed in both direct and indirect pathways, including reduced expression of A2a and D1 receptors markers (Dowie et al., 2009; Glass et al., 2004; Miller et al., 2014) and altered MSNs physiology (Andre et al., 2011; Barry et al., 2018; Goodliffe et al., 2018).

In addition, motor learning deficits and reduced rearing behavior are core symptoms present in HD models (Creus-Muncunill et al., 2019; Fernández-García et al., 2020; Hong et al., 2012; Pépin et al., 2016; Puigdellívol et al., 2015). Remarkably, we recently showed that selective optogenetic stimulation of M2 cortex-DLS projection restores motor learning, exploratory behavior and coordination in the R6/1 mouse model of HD (Fernández-García et al., 2020). However, the specific contributions of the distinct striatal subcircuits and its functional implications on locomotion and motor learning in HD are not yet known.

To delve into the contributions of the distinct striatal subcircuits to motor control, we employed optogenetic techniques to selectively stimulate D1 or A2a expressing neurons in either the DLS or DMS. We systematically evaluated the effects of the repeated optogenetic stimulation of the diverse subcircuits on locomotion, exploratory behavior and motor learning in WT and the R6/1 mouse model of HD. Better comprehension of the role of the distinct striatal subcircuits in motor behavior and, specifically, their involvement in HD will help to further understand motor control and to design effective therapeutic strategies.

2. Materials and methods

2.1. Animals

The transgenic R6/1 mice were used as mouse model of HD. R6/1 mouse express the exon-1 of mutant huntingtin with ~115–150 CAG repeats expansion and were originally acquired from The Jackson Laboratory (Bar Harbor, ME; (B6CBA-Tg(HDexon1)61Gpb/1 J; RRID: IMSR_JAX:002809) and maintained on a B6CBA background by breeding transgenic male mice with C57BL/6 J x CBA/J F1 females. At the time of the experiments, the length of CAG repeats was measured in six animals, which provided CAG repeats values ranging between 143 and 147. Heterozygous R6/1 male mice were crossed with heterozygous Adora2a-Cre+/− (Durieux et al., 2012) and heterozygous Drd1a-Cre+/− female (129S6.FVB(B6)-Tg(Drd1a-cre)AGsc/KndlJ, The Jackson Laboratory), both with Bl6 background) to obtain WT-Adora2a-Cre + (A2a-WT mice), R6/1-Adora2a-Cre + (A2a-HD mice), R6/1-Drd1-Cre + (D1-HD mice) and WT-Drd1a-Cre + (D1-WT mice), respectively. Due to the different background of the crossed mice, F2 inbred mice from the same litter, which include both genotypes, were used for all experiments. Genotypes were determined by polymerase chain reaction from ear biopsy. Mice groups (AAV-GFP / AAV-ChR2) were randomly assigned and behavioral data were recorded for analysis by microchip mouse number, blind to the experimenter. Mice were housed in groups of mixed genotypes under a 12:12 h light/dark cycle with access to water and food ad libitum, in a room kept at 19–22 °C and 40–60 % humidity. A maximum of 5 mice were housed together in a cage containing sawdust and enriched with wooden bricks and shredded paper. Experiments were conducted using 16–22 weeks-old male mice (surgeries performed at 16 week and behavior between 20 and 22 weeks). All animal procedures were conducted in accordance with the Spanish RD 53/2013 and European 2010/63/UE regulations for the care and use of laboratory animals and approved by the animal experimentation Ethics Committee of the Universitat de Barcelona (274/18) and Generalitat de Catalunya (10101). This study was in compliance with the ARRIVE guidelines.

2.2. Stereotaxic surgery

Stereotaxic surgery was performed in ~16-week-old male D1-HD, D1-WT, A2a-HD and A2a-WT mice under isoflurane anesthesia (5 % induction and 1.5 % maintenance). After fur shaving and scalp cleaned with ethanol and iodine, local anesthesia was applied (Lidocaine 2.5 % and Prilocaine 2.5 % EMLA, AstraZeneca) and a dose of 2 mg/kg of analgesic Metacam was injected subcutaneously. Small bilateral holes were drilled according to DLS or DMS coordinates from bregma and dura matter: DLS [+0.1 AP, ±2.2 L, −3.0 DV]; DMS [+0.5 AP, ±1.5 L, −3.0 DV] and double-floxed inverted (DIO) recombinant AAV-DIO encoding the channelrhodopsin-2 (ChR2) fused to enhanced yellow fluorescent protein (eYFP) (AAV1-EF1a-DIO-ChR2(E123A)-eYFP; Addgene catalog: #35507-AAV1) or eYFP as control (AAV1-EF1a-DIO-eYFP; Addgene catalog: #27056-AAV1) were injected. 0,5 μL of the AAV construct was injected in each hemisphere using 5 μl Hamilton syringe with a 33-gauge needle at 0.1 μl/min, followed by an additional 5 min period to allow diffusion and avoid reflux. Then, fiber-optic cannulas (MFC_200/240–0.22_3.5mm_ZF1.25_FLT; Doric Lenses) were implanted and fixed during surgery using dental cement (TAB 2000tm, Kerr Dental). All surgeries were performed 4 weeks before experiments were initiated to allow mice recovery and a stable expression of viral constructs. AAV expression and cannula implantation was validated post-mortem by immunofluorescence in sagittal sections of one hemisphere and mice were excluded from the analysis when AAV was not expressed and/or cannula was misplaced.

2.3. Optogenetic stimulation

Blue light was delivered from 473 nm diode-pumped solid-state blue laser (Laserglow) using a custom-made wave-form generator (Arduino) while mice were freely moving in the open field (OF) at 20, 21 and 22-weeks of age. Mice were placed in the OF and after 5 min, light stimulation was performed in a series of 10 trials of laser illumination and each trial alternated a 30 s period in which laser was ON [Cte illumination, ~5 mW (at tip of each fiber)], followed by a 60 s period in which laser was OFF, based on (Kravitz et al., 2010), then mice were left in the OF for 5 additional minutes.

2.4. Behavioral assessment

Behavioral tests were performed as previously described (Fernández-García et al., 2020). Animals were habituated to the experimental room for at least 1 h before testing and all apparatus were cleaned with water and dried between animals. Mice that experienced a seizure just before or during the test were excluded from the corresponding data and not included in the analyses.

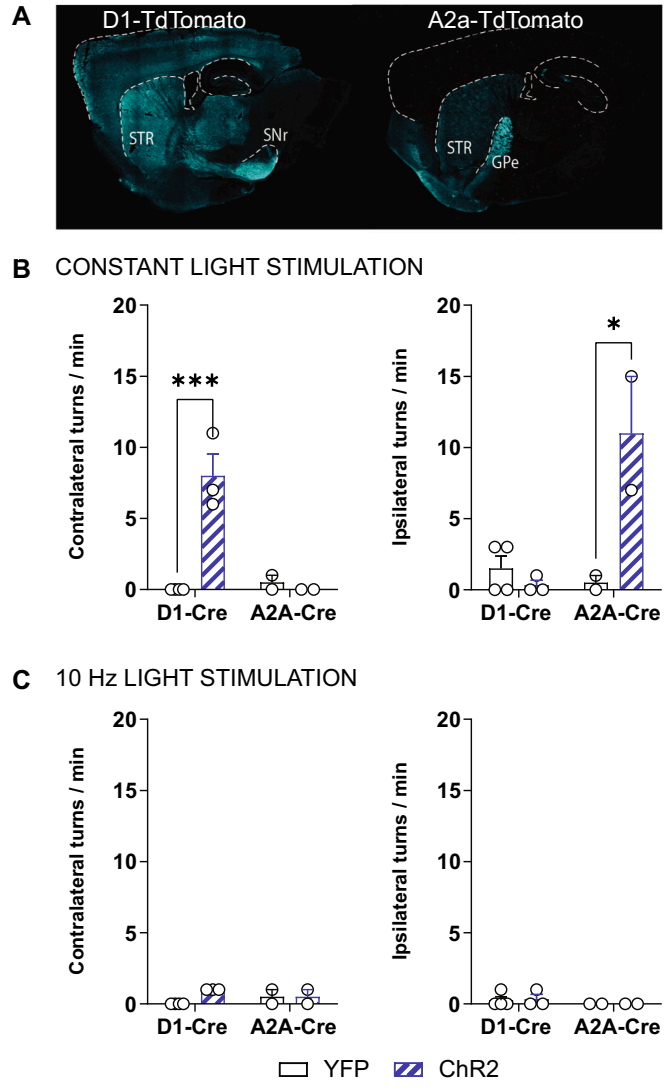

Fig. 1. Validation of D1-Cre and Adora2a-Cre mice and selection of optogenetic stimulation protocol. (A) Heterozygous Drd1a-Cre+/− (D1) and Adora2a-Cre+/− (A2a) male mice were crossed with homozygous Flox-TdTomato female to validate pathway specificity, resulting in 50 % D1-TdTomato and 50 % A2a-TdTomato mice. Tdtomato was constitutively expressed in all D1- and A2a-expressing cells (cyan). Within the striatum (STR), D1-expressing cells (left) project to the substantia nigra pars reticulata (SNr) and give rise to the direct pathway, whereas A2a-expressing cells (right) project to the globus pallidus externus (GPe) and give rise to the indirect pathway. (B—C) Optogenetic stimulation was delivered unilaterally to the DLS, and induction of circling behavior analyzed by the number of contralateral and ipsilateral turns/ min induced, using a 473 nm laser at (B) constant light stimulation, as in Kravitz et al., 2010 and at (C) 10 Hz light stimulation, as in Fernández-García et al. (2020). Data are represented as mean ± SEM. Number of mice per group: D1-Cre $n = 4$ and A2a-Cre $n = 2$ mice. *$p < 0.05$, ***$p < 0.001$. (For interpretation of the references to colour in this figure legend, the reader is referred to the web version of this article.)

2.4.1. Open field (OF)

Optogenetic stimulation was performed in the OF, which consists in a white square arena (40 × 40 × 30 cm3) with dim light (~20 lx). Mice were left in the center of the apparatus and allowed to freely explore the arena during a total of 25 min (5 min PRE-stimulation, 15 min TRAIN-stimulation (30s ON +60 OFF), 5 min POST-stimulation. Tracking and recording of mice were performed using SMART 3.0 software (Panlab).

2.4.2. Accelerating rotarod (ARR)

Motor learning was assessed using the rotarod apparatus at 21 weeks of age. Mice were placed on a motorized horizontal rod (30 mm diameter) with a rotation speed increasing from 4 to 40 rpm over 5 min. The test was performed four times per day during three consecutive days (12 trials in total) and latency to fall from the rod was measured for each trial. Different trials during the same day were separated by 1 h.

2.5. Immunohistochemistry

Intra-cardiac perfusion was performed with cold PBS and 4 % paraformaldehyde solution. Brains were post-fixed in 4 % paraformaldehyde for 24 h and dehydrated in a PBS/Sucrose gradient [from 15 % (48 h post-mortem) to 30 % (72 h post-mortem)] with 0.02 % Sodium Azide and kept at 4 °C. Sagittal sections were obtained at 30 μm with a vibratome (Leica VT1000 S) and cryopreserved [30 % Ethylene glycol, 30 % Glycerol, 25 % Tris HCl (pH = 7.5) and 15 % H2O miliQ] at −20 °C.

Viral injections were validated using anti-GFP (anti-Green Fluorescent Protein, 1:500, Invitrogen, #11122) as previously described (Fernández-García et al., 2020). Free-floating sections were washed in PBS and permeabilized and blocked for 15 min in PBS containing 0.3 % Triton X- 100 and 3 % Normal Goat Serum (NGS, Pierce Biotechnology). Sections were then washed again in PBS and incubated overnight at 4 °C with primary antibodies. The day after, slices were washed three times and then incubated 2 h rocking at RT with the secondary antibody goat anti-rabbit Cy3 (Cy3, 1:200, Jackson ImmunoResearch, West Grove, PA, USA). Brain slices were finally mounted on microscope slides using DAPI Fluoromount-G (SouthernBiotec). Fluorescence signal was detected using a Leica AF600 Fluorescence Microscope and mosaics were captured using a 20× objective with 1.6 magnification.

2.6. Statistical analysis

Results are expressed as mean ± SEM and data from individual mouse is represented by single points when possible. GraphPad Prism version 8.0.0. Software was used for statistical analyses. Statistical analyses included one-way ANOVA or two-way ANOVA analysis and followed by Bonferroni post-hoc test, with the factors used indicated in the results section and/or figure legends. Values were considered as statistically significant when $p < 0.05$.

3. Results

3.1. Light stimulation pattern differently modulates motor behavior in wild type mice

Aiming to understand how the distinct striatal subcircuits modulate motor activity, we combined the use of optogenetic tools and mice that express Cre under the D1 and A2a- promoter to target direct and indirect pathways of the striatum (Fig. 1A). Then, we transduced mice with an AAV expressing ChR2 (or its control YFP) under double-floxed inverse open reading frame (DIO) system in DLS to achieve opsin expression either in D1 or A2a expressing neurons. Fiber-optic cannulas were implanted in the same coordinates. Because different stimulation patterns could lead to different outcomes, we tested two light stimulation protocols based on previous studies: constant illumination (Kravitz et al., 2010) and 10 Hz light stimulation (Fernández-García et al., 2020). Constant illumination was able to induce contralateral circling in D1 DLS WT mice and ipsilateral circling in A2A DLS WT mice during stimulation (Fig. 1B), while 10 Hz stimulation was not able to induce clear behavioral effects (Fig. 1C). Thus, constant illumination pattern was selected as stimulation protocol for subsequent experiments.

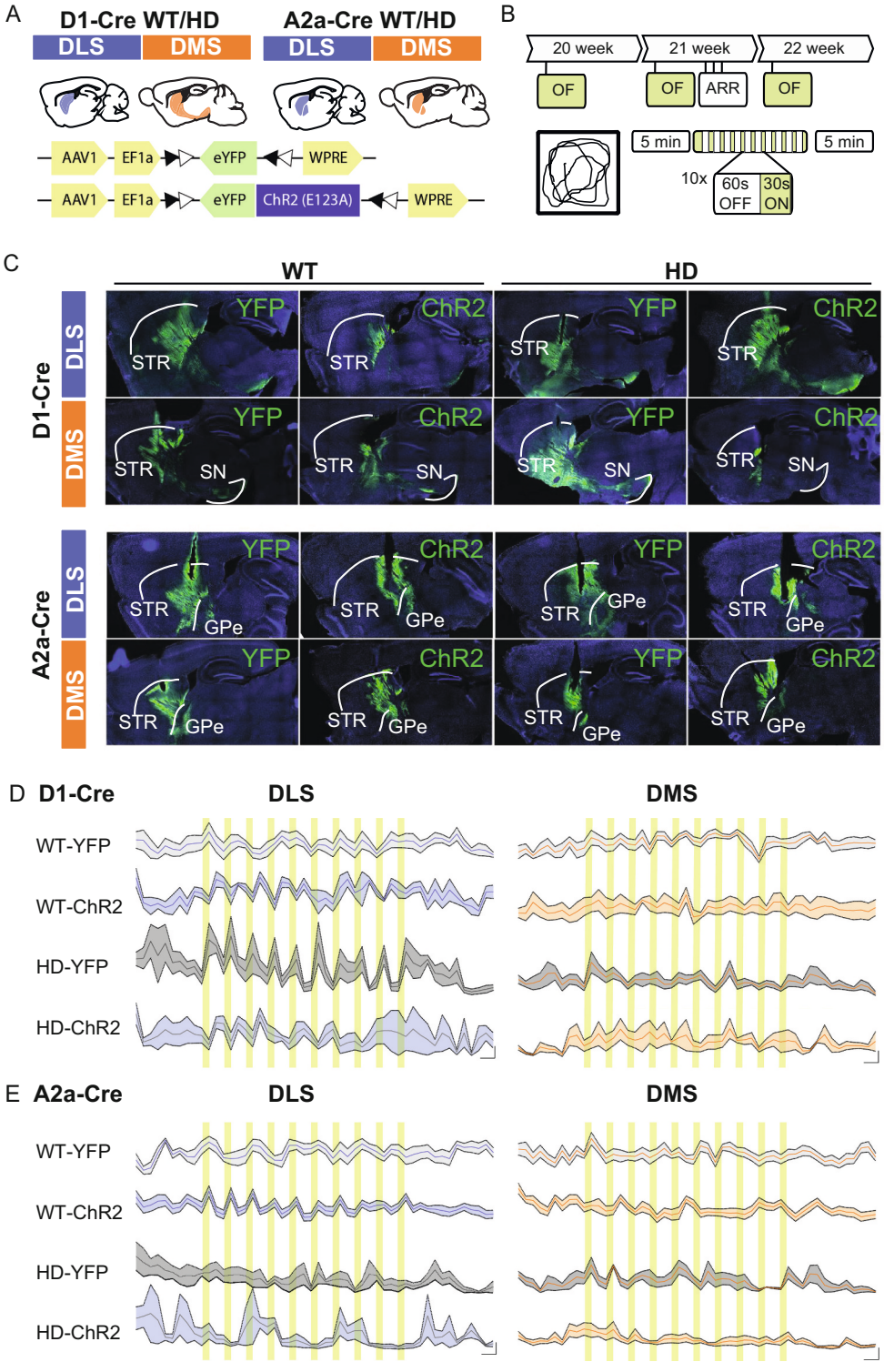

(caption on next page)

Fig. 2. Experimental protocol for the optogenetic stimulation of the direct or indirect pathways from DLS and DMS in WT and HD mice. (A) Schematic representation of the experimental mouse groups and AAV constructs. D1-Cre and A2a-Cre mice were crossed with R6/1 mice to obtain D1-WT, D1-HD, A2a-WT and A2a-HD mice. Then, AAV-YFP or AAV-ChR2 constructs were injected in the DLS or DMS of these mouse groups. (B) Optogenetic stimulation was performed during the three OF procedures at 20, 21 and 22 weeks of mouse age. The accelerating rotarod (ARR) task was performed after the 2nd stimulation day. Optogenetic stimulation started five minutes after the mice was placed in the OF and consisted of 10 trials of laser illumination and each trial alternated a 30 s period in which laser was ON [Constant illumination, ~5 mW] and 60 s period in which laser was OFF. Mice were left in the OF for an additional five minutes after the stimulation train. (C) Representative immunofluorescence images of AAV-ChR2 and AAV-YFP constructs expression (green), DAPI (blue) and cannula location at DLS or DMS of D1 WT, D1 HD, A2a WT and A2a HD mice. (D-E) Average distance travelled (cm) per min during the first OF session are represented for WT YFP, WT ChR2, HD YFP and HD ChR2 expressed in (D) direct pathway of the DLS (left panel) and DMS (right panel) and (E) indirect pathway from the DLS (left panel) and the DMS (right panel). The green shadow indicates the ten consecutive periods of 30 s in which laser was ON. Data are represented as mean ± SEM. Number of mice per group: Drd1-DLS-WT-YFP $n = 7$, Drd1-DLS-WT-ChR2 $n = 5$, Drd1-DLS-HD-YFP n = 5, Drd1-DLS-HD-ChR2 n = 4, Drd1-DMS-WT-YFP n = 7, Drd1-DMS-WT-ChR2 n = 5, Drd1-DMS-HD-YFP n = 5 and Drd1-DMS-HD-ChR2 $n = 3$; A2a-DLS-WT-YFP n = 7, A2a-DLS-WT-ChR2 $n = 12$, A2a-DLS-HD-YFP n = 4, A2a-DLS-HD-ChR2 n = 3, A2a-DMS-WT-YFP $n = 10$, A2a-DMS-WT-ChR2 n = 12, A2a-DMS-HD-YFP n = 4 and A2a-DMS-HD-ChR2 $n = 6$. Abbreviations: Globus Pallidus pars externa (GPe), Substantia nigra (SN) and Striatum (STR). (For interpretation of the references to colour in this figure legend, the reader is referred to the web version of this article.)

3.2. Optogenetic stimulation of the direct or indirect pathways from the DLS and DMS induces different locomotor responses in WT and HD mice

Based in our previous finding where optogenetic stimulation of M2 cortical afferences to the DLS improved motor phenotype in the R6/1 mouse model of HD (Fernández-García et al., 2020), we aimed to understand how selective activation of direct and indirect pathways in the DLS or DMS could show differential motor responses in WT and HD mice at same symptomatic stage. First, we crossed D1-Cre and A2a-Cre mice with R6/1 mice to obtain D1-WT, D1-HD, A2a-WT and A2a-HD mice. AAV-YFP or AAV-ChR2 was injected in the DLS or DMS of these mouse groups. Four weeks later, we evaluated how specific optogenetic activation of DMS and DLS striatal subcircuits affects motor behaviors in both WT and HD mice. The experimental procedure is detailed in Fig. 2. Mice were optogenetically stimulated once per week, during three consecutive weeks, while mice performed an OF task (Fig. 2B). The day after the second session of OF, mice performed the accelerated rotarod test to assess motor learning. DMS and DLS subcircuits were illuminated in a series of 10 trials during the OF, each trial alternated 30 s during which the laser was ON (constant illumination), followed by 60 s period during which the laser was OFF (Fig. 2B). Validation of correct viral expression and cannula implantation was assessed by immunofluorescence (Fig. 2C).

In bilaterally stimulated mice, the stimulation induced changes in locomotor activity throughout the OF. Fig. 2D-E shows the precise changes in locomotor activity every 30 s in D1 DLS, D1 DMS, A2a DLS and A2a DMS. Each panel shows the effects of WT and HD mice expressing either ChR2 or YFP. Our results show different activity profiles in the diverse striatal subcircuits and between WT and HD mice. Particularly, a clear increase in locomotion was observed in A2a DLS WT ChR2 expressing mice during light stimulation. However, our data also shows a clear light-dependent locomotor pattern in mice expressing both ChR2 and YFP, indicating that light per se might have an influence on these locomotor changes and could mask our results. Moreover, the profile of these changes decreased over time, suggesting certain habituation to the light and the open field.

Thus, to avoid light-dependent but not ChR2-dependent effects, and based on our previous study where optogenetic stimulation induced persistent behavioral effects across three open field sessions (Fernández-García et al., 2020), we decided to only quantify the effects on locomotion the 5 min before (PRE) and the 5 min after (POST) stimulation (Fig. 3). We evaluated locomotion effects using two-way ANOVA considering the three OF as repeated measurements and the different groups as factors for each of the subcircuits studied. During the 5 min PRE-stimulation, there were no significant differences in locomotor activity between WT-YFP, WT-CHR2, HD-YFP and HD-CHR2 groups over the three OF sessions for all the pathways analyzed except in mice in which optogenetic stimulation was performed in the indirect pathway from the DMS (Table 1). In this group, Bonferroni main group post-hoc comparisons showed that optogenetic stimulation increased locomotor activity in WT-CHR2 compared to WT-YPF.

Conversely, in the 5 min POST-stimulation, we clearly observed group effects in all conditions, as summarized in Table 1. Bonferroni main group post-hoc comparisons showed significantly reduced locomotion in HD mice in all conditions, compared to WT YFP. Optogenetic stimulation was unable to modulate locomotion in HD mice in any of the striatal subcircuits tested. Of note, locomotion was significantly induced in WT-CHR2 mice compared to WT-YPF mice when the direct pathway from the DLS was stimulated (Fig. 3A).

3.3. Optogenetic stimulation of the distinct striatal output pathways does not affect exploratory behavior in either WT or HD mice

We further evaluated the effects of the optogenetic stimulation on the rearing time (Fig. 4). In our previous study, optogenetic stimulation of DLS cortical inputs was able to increase rearing time over the different sessions, both before and after the stimulation, (Fernández-García et al., 2020). Thus, here we also compared the effect of optogenetic stimulation on total rearing time before (PRE) and after (POST) the stimulation and over the 3 sessions, for each of the striatal subcircuits tested: D1 DLS, D1 DMS, A2a DLS and A2a DMS.

Two-way ANOVA with OF test (day effect) as repeated measurements and group as factors showed that there are significant group effects for all experimental groups tested, as detailed in Table 1. However, Bonferroni main group comparisons post hoc test showed significant genotype effects, but not significant effect of CHR2 expressing groups compared to YFP expressing groups, indicating that the optogenetic stimulation of the diverse striatal subcircuits was not able to modulate rearing time in neither WT nor HD mice.

3.4. Optogenetic stimulation of the indirect pathway from the DLS increases motor learning in WT mice but not in HD mice

We then explored the effects of the distinct striatal output subcircuit stimulation on motor learning (Fig. 5). Motor learning was assessed by measuring the latency to fall from the accelerated rotarod, as previously described (Creus-Muncunill et al., 2019; Fernández-García et al., 2020; Puigdellívol et al., 2015). In our previous study, optogenetic stimulation of M2 cortex-DLS circuit was able to reverse the motor learning deficits observed in symptomatic R6/1 mice (Fernández-García et al., 2020). Here, HD mice showed reduced latency to fall compared to WT in all groups tested (Fig. 5), as expected. Notably, optogenetically stimulated WT mice increased the latency to fall from the rod when the stimulation was performed in the indirect pathway from DLS (Fig. 5C). Moreover, we quantified the area under the curve (AUC) for each experimental group (Fig. 5, right panel). One-way ANOVA showed significant group effects in all tested sub-circuits (D1 DLS: $(F(3,15) = 14.5, p = 0.0001)$; D1 DMS: $(F(3,16) = 11.6, p = 0.0003)$; A2a DLS: $(F(3,23) = 22.75, p \langle 0.0001)$ and A2A DMS: $(F(3,26) = 8.422, p = 0.0004)$. Bonferroni post-hoc test highlights that A2A DLS optogenetically stimulated WT mice (WT CHR2) increase motor learning performance compared to control (WT YFP) ($p = 0.05$), while all other significant group comparisons

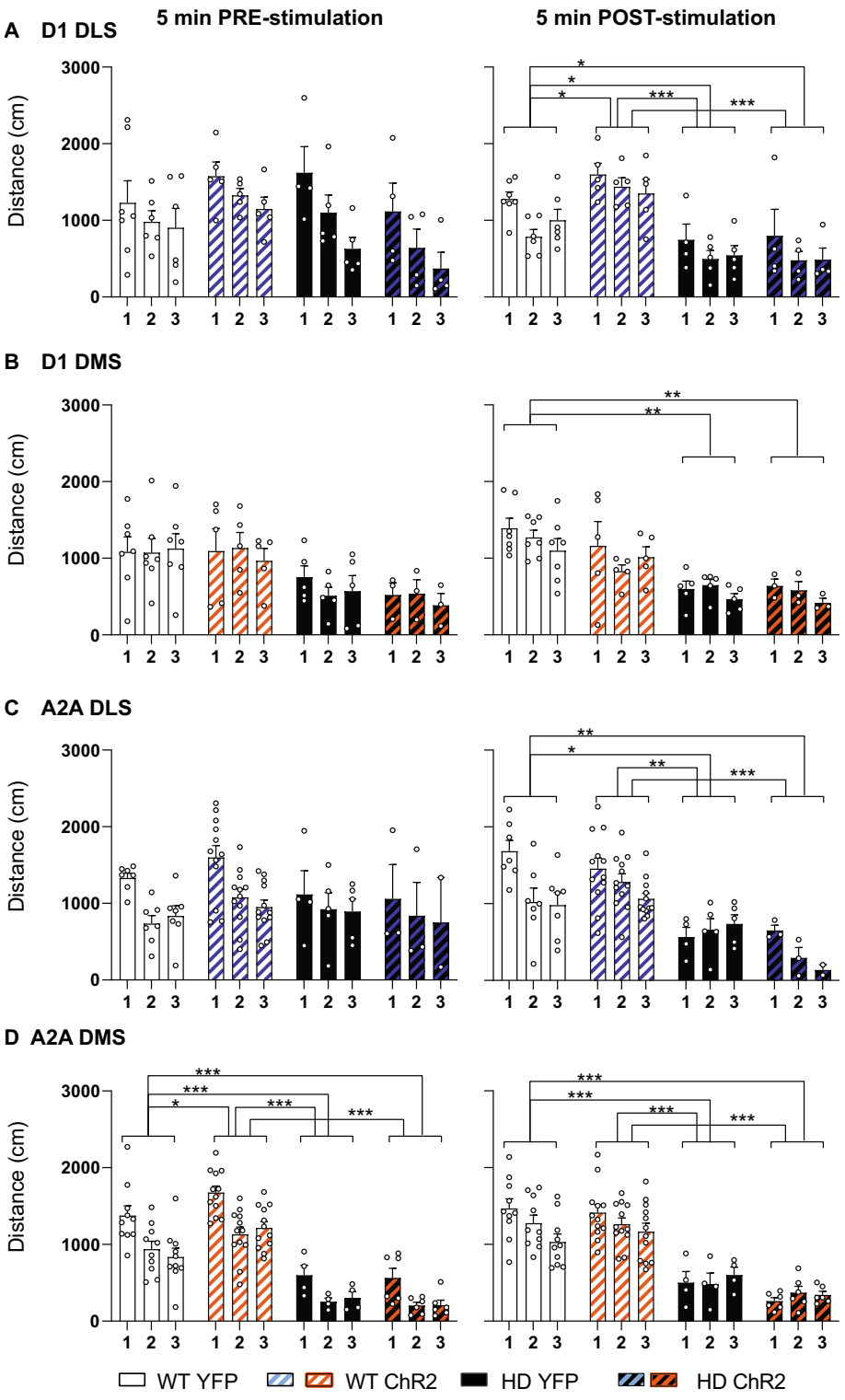

Fig. 3. Locomotor activity induced by optogenetic stimulation of the direct (D1) or indirect (A2a) pathways from DLS and DMS in WT and HD mice, over three open field sessions. The effects of ChR2 or YFP expressed in WT and HD mice on total distance travelled was compared before (5 min PRE, left panels) and after (5 min POST, right panels) the optogenetic stimulation for (A) direct pathway of the DLS (D1 DLS), (B) direct pathway from the DMS (D1 DMS), (C) indirect pathway from the DLS (A2a DLS) and (D) indirect pathway from the DMS (A2a DMS). A two-way ANOVA with AAV construct and genotype group as factors was performed, followed by main group Bonferroni post-hoc comparisons test. Each point represents data from an individual mouse and data are represented as mean ± SEM. Number of mice per group: Drd1-DLS-WT-YFP n = 7, Drd1-DLS-WT-ChR2 n = 5, Drd1-DLS-HD-YFP n = 6, Drd1-DLS-HD-ChR2 n = 4, Drd1-DMS-WT-YFP n = 7, Drd1-DMS-WT-ChR2 n = 5, Drd1-DMS-HD-YFP n = 5 and Drd1-DMS-HD-ChR2 n = 3; A2a-DLS-WT-YFP n = 7, A2a-DLS-WT-ChR2 n = 12, A2a-DLS-HD-YFP n = 5, A2a-DLS-HD-ChR2 n = 3, A2a-DMS-WT-YFP n = 10, A2a-DMS-WT-ChR2 n = 12, A2a-DMS-HD-YFP n = 4 and A2a-DMS-HD-ChR2 n = 6. *p < 0.05, **p < 0.01, ***p < 0.001.

Table 1
Locomotion and rearing time statistical effects between WT-YFP, WT-CHR2, HD-YFP, and HD-CHR2 groups across the three OF sessions.

		Locomotion		Rearing time	
Group	Factor	F(DFn, DFd)	*P* value	F(DFn, DFd)	P value
D1 DLS PRE	Day	F (2,30) = 18.94	**<0.0001***	F (2, 30) = 0.058	0.9438
	Group	F (3, 18) = 1.532	0.2404	F (3, 18) = 3.958	**0.0249***
	Day/ Group	F (6, 30) = 0.855	0.5384	F (6, 30) = 0.296	0.9342
D1 DLS POST	Day	F (2, 30) = 5.225	**0.0113***	F (2, 30) = 4.241	**0.0239***
	Group	F (3, 18) = 16.62	**<0.0001***	F (3, 18) = 7.610	**0.0017***
	Day/ Group	F (6, 30) = 0.343	0.9086	F (6, 30) = 0.932	0.4867
D1 DMS PRE	Day	F (2,32) = 0.897	0.4180	F (2, 32) = 2.046	0.1459
	Group	F (3, 16) = 2.644	0.0846	F (3, 16) = 4.882	**0.0135***
	Day/ Group	F (6, 32) = 0.699	0.6521	F (6, 32) = 1.752	0.1411
D1 DMS POST	Day	F (2, 32) = 2.740	0.0797	F (2, 32) = 3.230	0.0527
	Group	F (3, 16) = 9.375	**0.0008***	F (3, 16) = 5.995	**0.0061***
	Day/ Group	F (6, 32) = 0.797	0.5795	F (6, 32) = 1.673	0.1599
A2A DLS PRE	Day	F (2, 44) = 8.768	**0.0006***	F (2, 44) = 0.471	0.6274
	Group	F (3,23) = 0.927	0.4433	F (3, 23) = 3.515	**0.0312***
	Day/ Group	F (6, 44) = 1.143	0.3538	F (6, 44) = 1.472	0.2101
A2A DLS POST	Day	F (2, 44) = 8.962	**0.0005***	F (2, 44) = 0.071	0.9316
	Group	F (3, 23) = 11.26	**<0.0001***	F (3, 23) = 8.979	**0.0004***
	Day/ Group	F (6, 44) = 2.732	**0.0241***	F (6, 44) = 0.099	0.9962
A2A DMS PRE	Day	F (2, 56) = 21.17	**<0.0001***	F (2, 56) = 1.800	0.1748
	Group	F (3, 28) = 45.28	**<0.0001***	F (3, 28) = 10.45	**<0.0001***
	Day/ Group	F (6, 56) = 0.480	0.8208	F (6, 56) = 0.387	0.8840
A2A DMS POST	Day	F (2, 56) = 1.837	0.1688	F (2, 56) = 0.389	0.6794
	Group	F (3, 28) = 29.55	**<0.0001***	F (3, 28) = 15.45	**<0.0001***
	Day/ Group	F (6, 56) = 2.178	0.0586	F (6, 56) = 0.595	0.7332

Summary of two-way ANOVA statistical analysis of locomotion and rearing time before (PRE) and after (POST) optogenetic stimulation for each striatal subcircuit group: D1 DLS, D1 DMS, A2a DLS and A2a DMS. The four groups were compared considering the three stimulation sessions (day) as repeated measures for each subcircuit analyzed: WT YFP, WT CHR2, HD YFP and HD ChR2.

reflect genotype differences in all subcircuits evaluated. As for locomotion and exploratory behavior, optogenetic stimulation did not modulate motor learning in any HD mouse group.

4. Discussion

Alterations in the basal ganglia circuitry have been long associated to the motor symptoms in HD. Building on our previous study, which demonstrated that optogenetic stimulation of cortical afferences to the DLS reversed motor learning and exploratory behavior deficits in HD mice (Fernández-García et al., 2020), we systematically evaluated the effects of selective optogenetic stimulation of the direct and indirect pathway from DLS and DMS on locomotion, exploratory behavior and motor learning in WT and HD mice. Our data shows that unilateral optogenetic stimulation reliably induced rotations, demonstrating the effectiveness of the optogenetic stimulation approach. However, bilateral stimulation produced only subtle motor effects in WT mice and failed to modify the motor phenotype in HD mice.

These findings suggest that the relationship between optogenetic activation of D1 or A2a expressing cells and movement may be more complex than previously thought (Kravitz et al., 2010). While lesion studies have shown that specific ablation of the direct pathway reduces locomotion and ablation of the indirect pathway increases it (Durieux et al., 2012), our data indicate that the effects of pathway activation may not be as straightforward.

The stimulation of the distinct striatal subcircuits with optogenetics was not sufficient to modulate motor responses in HD mice, despite unilateral stimulation being able to induce rotational behavior also in HD mice (data not shown). Thus, our present results contrast with our previous study (Fernández-García et al., 2020), where M2 cortex – DLS optogenetic stimulation was able to increase locomotion, rearings and motor learning in symptomatic R6/1 mice. The fact that direct stimulation of MSNs in the DLS (present results) does not modulate any of these behaviors indicate that acting on cortico-striatal circuitry (Fernández-García et al., 2020) rather than directly in the striatum is a better strategy to ameliorate motor symptoms in HD. Moreover, these results agree with the idea that cortico-striatal terminals re-organization is needed for motor learning (Kupferschmidt et al., 2017).

Interestingly, altered responses in HD mouse models are observed upon dopamine signaling modulation, such as locomotor activity (Pineda et al., 2005), long-term potentiation (Kung et al., 2007) and expression of early genes (Spektor et al., 2002). Indeed, synergistic actions of glutamate and dopamine have been described, and dopamine potentiates glutamate-induced effects on calcium responses and induced apoptosis in HD (Tang et al., 2007). Therefore, it could be that concomitant activation of glutamate and dopamine pathways is needed to modulate these motor behaviors, which is not the case when using our optogenetic approach.

Of note, we also showed that different patterns of stimulation have differential effects on the rotational behavior. Accordingly, it has been shown that the optogenetic stimulation pattern could affect mean velocity (Freeze et al., 2013). Moreover, it has been shown that A2A-dependent motor suppression relies on sufficient striatal collateral inhibition rather than indirect pathway activation (Isett et al., 2023). Therefore, we cannot exclude that a different pattern of light could lead to differential motor effects, as the pattern of activity and the extent of striatal volume stimulated, inhibited or lesioned seems to tightly modulate the motor responses observed by striatal subcircuits stimulation.

Regarding motor learning, our findings reveal that prior optogenetic stimulation of A2a-expressing neurons in the DLS enhances performance on the accelerated rotarod task in WT mice. This aligns with previous research suggesting that extensive training induces long-term potentiation (LTP) onto A2a- expressing neurons from the DLS (Yin et al., 2009). Yet, several authors have shown that the acquisition of a skill requires a complex re-organization of MSNs neuronal activity in both DLS and DMS (Badreddine et al., 2022; Durieux et al., 2012; Kupferschmidt et al., 2017; Yin et al., 2009), and the involvement of pre-synaptic cortical inputs is required for motor learning (Kupferschmidt et al., 2017). Thus, while A2A might have a role in rotarod test performance, the involvement of the other subcircuits in motor learning still requires further investigation.

One of the limitations of the study is the low number of mice per group. While the group size was sufficient to demonstrate that optogenetic stimulation of the direct and indirect pathways in the DLS and DMS, respectively, induces subtle locomotor and motor learning responses in healthy mice, smaller effects on these behaviors may have been underestimated. However, the data did not reveal any small change or trend suggesting phenotype modulation in HD mice, which contrast

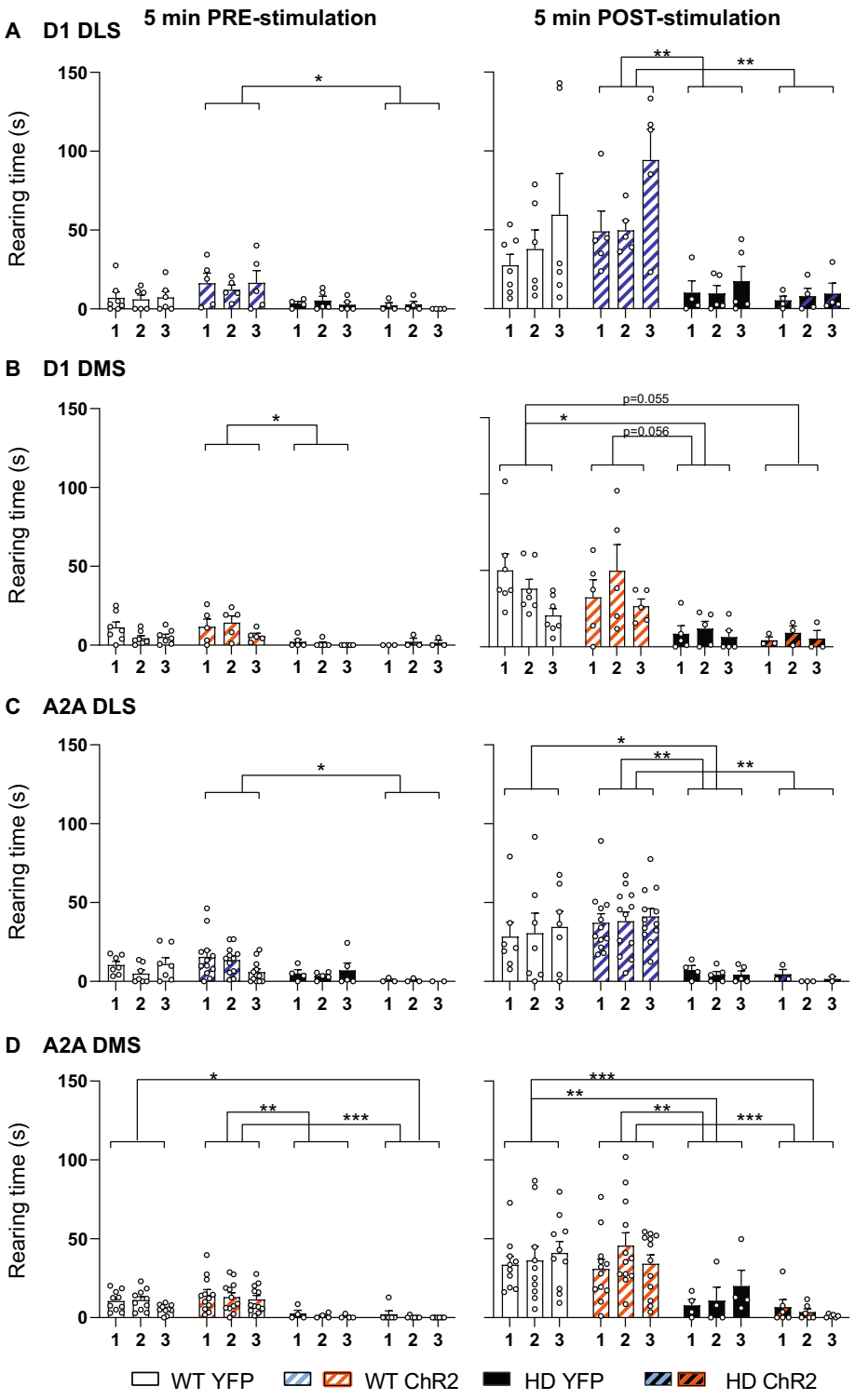

Fig. 4. Exploratory behavior induced by optogenetic stimulation of the direct (D1) or indirect (A2a) pathways from DLS and DMS in WT and HD mice, over three open field sessions. The effects of ChR2 or YFP expressed in WT and HD mice on total rearing time was compared before (5 min PRE, left panels) and after (5 min POST, right panels) the optogenetic stimulation for (A) direct pathway of the DLS (D1 DLS), (B) direct pathway from the DMS (D1 DMS), (C) indirect pathway from the DLS (A2a DLS) and (D) indirect pathway from the DMS (A2a DMS). A two-way ANOVA with AAV construct and genotype group as factors was performed, followed by main group Bonferroni post-hoc comparisons test. Each point represents data from an individual mouse and data are represented as mean ± SEM. Number of mice per group: Drd1-DLS-WT-YFP n = 7, Drd1-DLS-WT-ChR2 n = 5, Drd1-DLS-HD-YFP n = 6, Drd1-DLS-HD-ChR2 n = 4, Drd1-DMS-WT-YFP n = 7, Drd1-DMS-WT-ChR2 n = 5, Drd1-DMS-HD-YFP n = 5 and Drd1-DMS-HD-ChR2 n = 3; A2a-DLS-WT-YFP n = 7, A2a-DLS-WT-ChR2 n = 12, A2a-DLS-HD-YFP n = 5, A2a-DLS-HD-ChR2 n = 3, A2a-DMS-WT-YFP n = 10, A2a-DMS-WT-ChR2 n = 12, A2a-DMS-HD-YFP n = 4 and A2a-DMS-HD-ChR2 n = 6. *$p < 0.05$, **$p < 0.01$, ***$p < 0.001$.

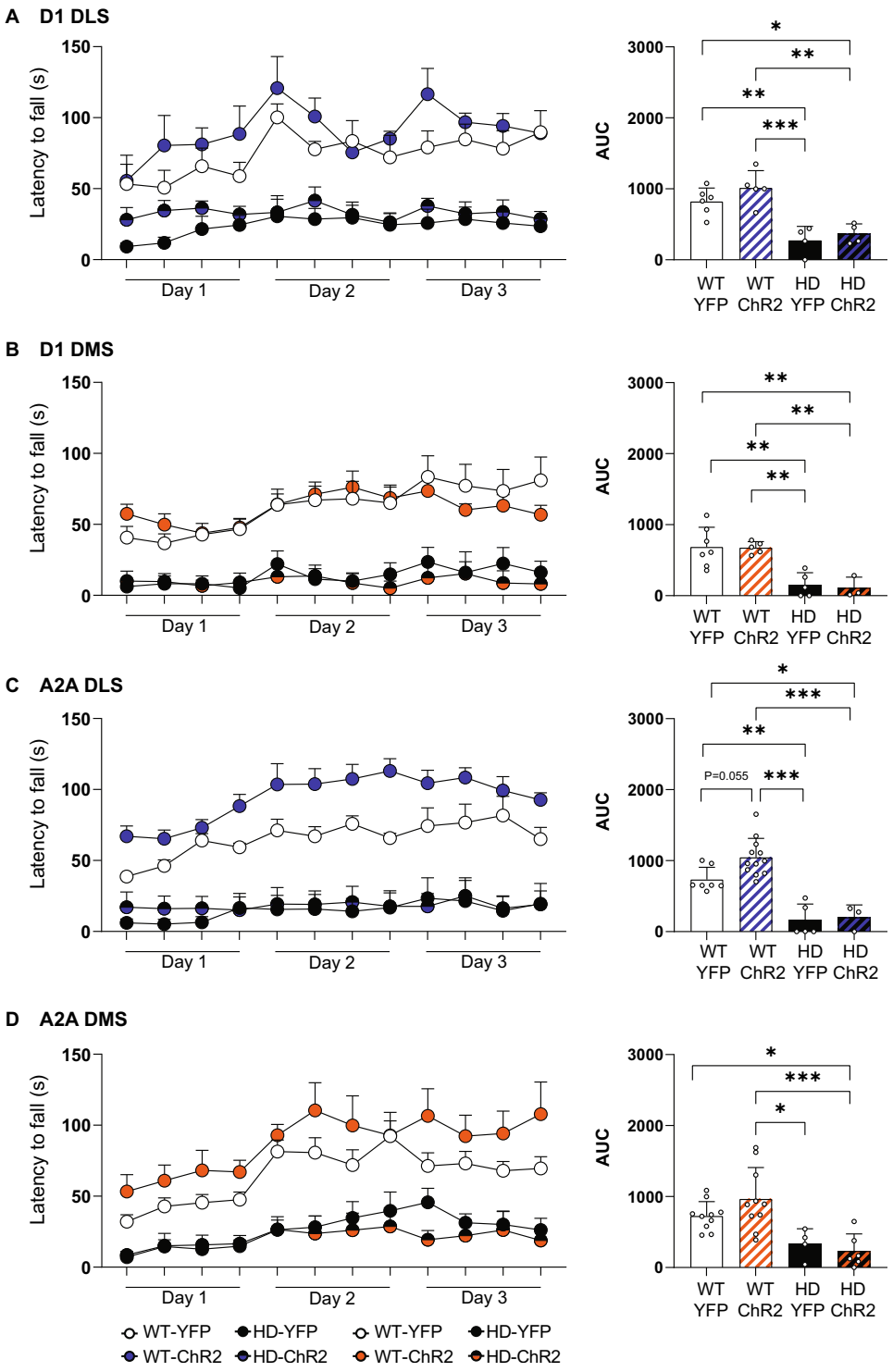

Fig. 5. Effects of optogenetic stimulation of the direct (D1) or indirect (A2a) pathways from DLS and DMS in WT and HD mice on motor learning. Latency to fall in the ARR was measured after two sessions of optogenetic stimulation of (A) direct pathway of the DLS (D1 DLS), (B) direct pathway from the DMS (D1 DMS), (C) indirect pathway from the DLS (A2a DLS) and (D) indirect pathway from the DMS (A2a DMS). Additionally, the area under the curve (AUC) was calculated. AUC data were analyzed by one-way ANOVA, followed by Bonferroni's mean group multiple comparison test as post-hoc. Each point represents data from an individual mouse and data are represented as mean ± SEM. Number of mice per group: Drd1-DLS-WT-YFP n = 6, Drd1-DLS-WT-ChR2 n = 5, Drd1-DLS-HD-YFP n = 4, Drd1-DLS-HD-ChR2 n = 4, Drd1-DMS-WT-YFP n = 7, Drd1-DMS-WT-ChR2 n = 5, Drd1-DMS-HD-YFP n = 5 and Drd1-DMS-HD-ChR2 n = 3; A2a-DLS-WT-YFP n = 7, A2a-DLS-WT-ChR2 n = 12, A2a-DLS-HD-YFP n = 5, A2a-DLS-HD-ChR2 n = 3, A2a-DMS-WT-YFP n = 10, A2a-DMS-WT-ChR2 n = 10, A2a-DMS-HD-YFP n = 4 and A2a-DMS-HD-ChR2 n = 6. *$p < 0.05$, **$p < 0.01$, ***$p < 0.001$.

with our early findings (Fernández-García et al., 2020), where cortico-striatal optogenetic stimulation produce robust effects. Another limitation is the use of only males in the study. We cannot discard that the effects of optogenetic stimulation might be different between males and females, especially as dimorphic dopaminergic dysfunction has been described in the R6/1 mouse model of HD (Renoir et al., 2014). Also, we cannot exclude that the optogenetic stimulation at earlier time could produce differential effects. However, we selected to study the effects in symptomatic male mice in order to compare the results with our previous study (Fernández-García et al., 2020).

In summary, our results highlight that optogenetic stimulation of direct and indirect pathways from DLS and DMS induces subtle locomotor and motor learning responses in healthy mice, favoring the idea that the orchestrated activity of the distinct striatal subcircuits and its dopamine and glutamate inputs is necessary to modulate these behaviors. Moreover, the lack of responses by optogenetic stimulation in HD mice, together with our previous results showing restoration of spontaneous behavior, motor learning and coordination (Fernández-García et al., 2020), suggests that strategies involving cortico-striatal circuits, rather than direct striatal stimulation might be a better therapeutic opportunity for treating motor symptoms in HD.

Funding

This research is part of NEUROPA and GlioLight project. The NEUROPA Project has received funding from the European Union's Horizon 2020 Research and Innovation Program under Grant Agreement No. 863214 (M.M.). The GlioLight project has received funding from the European Innovation Council under grant Agreement 101129705 (M. M.). This study was supported by grants from the Ministerio de Ciencia y Innovación (Spain), under projects CNS2023–143999 (MM.), PID2021-124896OA-I00 (M.M.), no. PID2020-119386RB-I00 (J.A. and M.J.R.), no. PID2021-122258OB-I00 (A.G) and no. AEI/10.13039/501100011033/ (A.G.); Instituto de Salud Carlos III, Ministerio de Ciencia, Innovación y Universidades and European Regional Development Fund (ERDF) [CIBERNED, to J.A.], Spain. Also, the project has been supported by María de Maeztu Unit of Excellence (CEX2021–001159), Institute of Neurosciences of the University of Barcelona, Ministry of Science, Innovation, and Universities and Universities and from the Agència de Gestió d'Ajuts Universitaris i de Recerca (AGAUR, Catalunya) (2021SGR01086).

CRediT authorship contribution statement

Sara Conde-Berriozabal: Writing – review & editing, Writing – original draft, Methodology, Investigation, Formal analysis, Data curation, Conceptualization. **Laia Sitjà-Roqueta:** Writing – review & editing, Methodology, Investigation. **Esther García-García:** Writing – review & editing, Methodology, Investigation. **Lia García-Gilabert:** Writing – review & editing, Methodology, Investigation. **Anna Sancho-Balsells:** Writing – review & editing, Methodology, Investigation. **Sara Fernández-García:** Writing – review & editing, Methodology, Investigation. **Ened Rodriguez-Urgellés:** Methodology, Investigation. **Albert Giralt:** Writing – review & editing, Resources, Methodology, Investigation, Funding acquisition. **Anna Castañé:** Writing – review & editing, Formal analysis, Data curation. **Manuel J. Rodríguez:** Writing – review & editing, Funding acquisition, Formal analysis, Data curation, Conceptualization. **Jordi Alberch:** Writing – review & editing, Funding acquisition, Conceptualization. **Mercè Masana:** Writing – review & editing, Writing – original draft, Validation, Supervision, Methodology, Investigation, Funding acquisition, Formal analysis, Data curation, Conceptualization.

Declaration of competing interest

The authors declare that they have no known competing financial interests or personal relationships that could have appeared to influence the work reported in this paper.

Acknowledgements

We are very grateful to Maria Teresa Muñoz, Ana Maria Lopez, Silvia Artigas and Albert Coll for excellent technical support. We are also grateful to the staff of the Confocal Microscopy Service and the Animal Experimental Unit of the Scientific and Technological Centers of the University of Barcelona (CCiTUB).

Data availability

The datasets used and/or analyzed during the current study are available from the corresponding author upon reasonable request.

References

Andre, V.M., Cepeda, C., Fisher, Y.E., Huynh, M., Bardakjian, N., Singh, S., Yang, X.W., Levine, M.S., 2011. Differential electrophysiological changes in striatal output neurons in Huntington's disease. J. Neurosci. 31, 1170–1182. https://doi.org/10.1523/JNEUROSCI.3539-10.2011.

Badreddine, N., Zalcman, G., Appaix, F., Becq, G., Tremblay, N., Saudou, F., Achard, S., Fino, E., 2022. Spatiotemporal reorganization of corticostriatal networks encodes motor skill learning. Cell Rep. 39. https://doi.org/10.1016/j.celrep.2022.110623.

Barry, J., Akopian, G., Cepeda, C., Levine, M.S., 2018. Striatal direct and indirect pathway output structures are differentially altered in mouse models of Huntington's disease. J. Neurosci. 38, 4678–4694. https://doi.org/10.1523/jneurosci.0434-18.2018.

Creus-Muncunill, J., Badillos-Rodríguez, R., Garcia-Forn, M., Masana, M., Barriga, G.G. D., Guisado-Corcoll, A., Alberch, J., Malagelada, C., Delgado-García, J.M., Gruart, A., Pérez-Navarro, E., 2019. Increased translation as a novel pathogenic mechanism in Huntington's disease. Brain 142, 3158–3175. https://doi.org/10.1093/brain/awz230.

Cui, G., Jun, S.B., Jin, X., Pham, M.D., Vogel, S.S., Lovinger, D.M., Costa, R.M., 2013. Concurrent activation of striatal direct and indirect pathways during action initiation. Nature 494, 238–242. https://doi.org/10.1038/NATURE11846.

Deng, Y.P., Albin, R.L., Penney, J.B., Young, A.B., Anderson, K.D., Reiner, A., 2004. Differential loss of striatal projection systems in Huntington's disease: a quantitative immunohistochemical study. J. Chem. Neuroanat. 27, 143–164. https://doi.org/10.1016/J.JCHEMNEU.2004.02.005.

Dowie, M.J., Bradshaw, H.B., Howard, M.L., Nicholson, L.F.B., Faull, R.L.M., Hannan, A. J., Glass, M., 2009. Altered CB1 receptor and endocannabinoid levels precede motor symptom onset in a transgenic mouse model of Huntington's disease. Neuroscience 163, 456–465. https://doi.org/10.1016/j.neuroscience.2009.06.014.

Durieux, P.F., Schiffmann, S.N., De Kerchove D'Exaerde, A., 2012. Differential regulation of motor control and response to dopaminergic drugs by D1R and D2R neurons in distinct dorsal striatum subregions. EMBO J. 31, 640–653. https://doi.org/10.1038/emboj.2011.400.

Fernández-García, S., Conde-Berriozabal, S., García-García, E., Gort-Paniello, C., Bernal-Casas, D., Barriga, G.G.-D., López-Gil, J., Muñoz-Moreno, E., Sòria, G., Campa, L., Artigas, F., Rodriguez, M., Alberch, J., Masana, M., 2020. M2 Cortex-Dorsolateral Striatum Stimulation Reverses Motor Symptoms and Synaptic Deficits in Huntington's Disease, pp. 1–24. https://doi.org/10.1101/2020.04.08.032359.

Freeze, B.S., Kravitz, A.V., Hammack, N., Berke, J.D., Kreitzer, A.C., 2013. Control of basal ganglia output by direct and indirect pathway projection neurons. J. Neurosci. 33, 18531–18539. https://doi.org/10.1523/JNEUROSCI.1278-13.2013.

Galvan, L., André, V.M., Wang, E.A., Cepeda, C., Levine, M.S., 2012. Functional differences between direct and indirect striatal output pathways in Huntington's disease. J. Huntingtons. Dis. 1, 17–25. https://doi.org/10.3233/JHD-2012-120009.

Glass, M., Dragunow, M., Faull, R.L.M., 2000. The Pattern of Neurodegeneration in Huntington's Disease: A Comparative Study of Cannabinoid, Dopamine, Adenosine and GABA a Receptor Alterations in the Human Basal Ganglia in Huntington's Disease.

Glass, M., Van Dellen, A., Blakemore, C., Hannan, A.J., Faull, R.L.M., 2004. Delayed onset of Huntington's disease in mice in an enriched environment correlates with delayed loss of cannabinoid CB1 receptors. Neuroscience 123, 207–212. https://doi.org/10.1016/S0306-4522(03)00595-5.

Goodliffe, J.W., Song, H., Rubakovic, A., Chang, W., Medalla, M., Weaver, C.M., Luebke, J.I., 2018. Differential changes to D1 and D2 medium spiny neurons in the 12-month-old Q175+/− mouse model of Huntington's disease. PLoS One 13, e0200626. https://doi.org/10.1371/journal.pone.0200626.

Hintiryan, H., Foster, N.N., Bowman, I., Bay, M., Song, M.Y., Gou, L., Yamashita, S., Bienkowski, M.S., Zingg, B., Zhu, M., Yang, X.W., Shih, J.C., Toga, A.W., Dong, H.W., 2016. The mouse cortico-striatal projectome. Nat. Neurosci. 19, 1100–1114. https://doi.org/10.1038/nn.4332.

Hong, S.L., Cossyleon, D., Hussain, W.A., Walker, L.J., Barton, S.J., Rebec, G.V., 2012. Dysfunctional behavioral modulation of Corticostriatal communication in the R6/2 mouse model of Huntington's disease. PLoS One 7, e47026. https://doi.org/10.1371/journal.pone.0047026.

Hunnicutt, B.J., Jongbloets, B.C., Birdsong, W.T., Gertz, K.J., Zhong, H., Mao, T., 2016. A comprehensive excitatory input map of the striatum reveals novel functional organization. Elife 5. https://doi.org/10.7554/eLife.19103.

Isett, B.R., Nguyen, K.P., Schwenk, J.C., Yurek, J.R., Snyder, C.N., Vounatsos, M.V., Adegbesan, K.A., Ziausyte, U., Gittis, A.H., 2023. The indirect pathway of the basal ganglia promotes transient punishment but not motor suppression. Neuron 111, 2218–2231.e4. https://doi.org/10.1016/J.NEURON.2023.04.017.

Kravitz, A.V., Freeze, B.S., Parker, P.R.L., Kay, K., Thwin, M.T., Deisseroth, K., Kreitzer, A.C., 2010. Regulation of parkinsonian motor behaviours by optogenetic control of basal ganglia circuitry. Nature 466, 622–626. https://doi.org/10.1038/nature09159.

Kung, V.W.S., Hassam, R., Morton, A.J., Jones, S., 2007. Dopamine-dependent long term potentiation in the dorsal striatum is reduced in the R6/2 mouse model of Huntington's disease. Neuroscience 146, 1571–1580. https://doi.org/10.1016/J.NEUROSCIENCE.2007.03.036/ASSET/DC343E92-FF57-420F-BEB6-02808DF9D662/MAIN.ASSETS/GR6.SML.

Kupferschmidt, D.A., Juczewski, K., Cui, G., Johnson, K.A., Lovinger, D.M., 2017. Parallel, but dissociable, processing in discrete Corticostriatal inputs encodes skill learning. Neuron 96. https://doi.org/10.1016/j.neuron.2017.09.040, 476–489.e5.

Lee, J., Wang, W., Sabatini, B.L., 2020. Anatomically segregated basal ganglia pathways allow parallel behavioral modulation. Nat. Neurosci. 23, 1388–1398. https://doi.org/10.1038/s41593-020-00712-5.

Lerner, T.N., Shilyansky, C., Davidson, T.J., Evans, K.E., Beier, K.T., Zalocusky, K.A., Crow, A.K., Malenka, R.C., Luo, L., Tomer, R., Deisseroth, K., 2015. Intact-brain analyses reveal distinct information carried by SNc dopamine subcircuits. Cell 162, 635–647. https://doi.org/10.1016/j.cell.2015.07.014.

MacDonald, M.E., Ambrose, C.M., Duyao, M.P., Myers, R.H., Lin, C., Srinidhi, L., Barnes, G., Taylor, S.A., James, M., Groot, N., MacFarlane, H., Jenkins, B., Anderson, M.A., Wexler, N.S., Gusella, J.F., Bates, G.P., Baxendale, S., Hummerich, H., Kirby, S., North, M., Youngman, S., Mott, R., Zehetner, G., Sedlacek, Z., Poustka, A., Frischauf, A.M., Lehrach, H., Buckler, A.J., Church, D., Doucette-Stamm, L., O'Donovan, M.C., Riba-Ramirez, L., Shah, M., Stanton, V.P., Strobel, S.A., Draths, K.M., Wales, J.L., Dervan, P., Housman, D.E., Altherr, M., Shiang, R., Thompson, L., Fielder, T., Wasmuth, J.J., Tagle, D., Valdes, J., Elmer, L., Allard, M., Castilla, L., Swaroop, M., Blanchard, K., Collins, F.S., Snell, R., Holloway, T., Gillespie, K., Datson, N., Shaw, D., Harper, P.S., 1993. A novel gene containing a trinucleotide repeat that is expanded and unstable on Huntington's disease chromosomes. Cell 72, 971–983. https://doi.org/10.1016/0092-8674(93)90585-E.

Miller, S., Hill Della Puppa, G., Reidling, J., Marcora, E., Thompson, L.M., 2014. Comparison of phosphodiesterase 10A, dopamine receptors D1 and D2 and dopamine transporter ligand binding in the striatum of the R6/2 and BACHD mouse models of Huntington's disease. J. Huntingtons. Dis. 3, 333–341. https://doi.org/10.3233/JHD-140129.

Pépin, J., Francelle, L., Carrillo-de Sauvage, M.A., de Longprez, L., Gipchtein, P., Cambon, K., Valette, J., Brouillet, E., Flament, J., 2016. In vivo imaging of brain glutamate defects in a knock-in mouse model of Huntington's disease. Neuroimage 139, 53–64. https://doi.org/10.1016/j.neuroimage.2016.06.023.

Pineda, J.R., Canals, J.M., Bosch, M., Adell, A., Mengod, G., Artigas, F., Ernfors, P., Alberch, J., 2005. Brain-derived neurotrophic factor modulates dopaminergic deficits in a transgenic mouse model of Huntington's disease. J. Neurochem. 93, 1057–1068. https://doi.org/10.1111/j.1471-4159.2005.03047.x.

Puigdellívol, M., Cherubini, M., Brito, V., Giralt, A., Suelves, N., Ballesteros, J., Zamora-Moratalla, A., Martín, E.D., Eipper, B.A., Alberch, J., Ginés, S., 2015. A role for Kalirin-7 in corticostriatal synaptic dysfunction in Huntington's disease. Hum. Mol. Genet. 24, 7265–7285. https://doi.org/10.1093/hmg/ddv426.

Reiner, A., Albin, R.L., Anderson, K.D., D'Amato, C.J., Penney, J.B., Young, A.B., 1988. Differential loss of striatal projection neurons in Huntington disease. Proc. Natl. Acad. Sci. USA 85, 5733–5737. https://doi.org/10.1073/pnas.85.15.5733.

Renoir, T., Argyropoulos, A., Chevarin, C., Lanfumey, L., Hannan, A.J., 2014. Sexually dimorphic dopaminergic dysfunction in a transgenic mouse model of Huntington's disease. Pharmacol. Biochem. Behav. 127, 15–20. https://doi.org/10.1016/J.PBB.2014.10.004.

Richfield, E.K., O'Brien, C.F., Eskin, T., Shoulson, I., 1991. Heterogeneous dopamine receptor changes in early and late Huntington's disease. Neurosci. Lett. 132, 121–126. https://doi.org/10.1016/0304-3940(91)90448-3.

Sapp, E., Ge, P., Aizawa, H., Bird, E., Penney, J., Young, A.B., Vonsattel, J.P., Difiglia, M., 1995. Evidence for a preferential loss of enkephalin immunoreactivity in the external globus pallidus in low grade Huntington's disease using high resolution image analysis. Neuroscience 64, 397–404. https://doi.org/10.1016/0306-4522(94)00427-7.

Spektor, B.S., Miller, D.W., Hollingsworth, Z.R., Kaneko, Y.A., Solano, S.M., Johnson, J. M., Penney, J.B., Young, A.B., Luthi-Carter, R., 2002. Differential D1 and D2 receptor-mediated effects on immediate early gene induction in a transgenic mouse model of Huntington's disease. Mol. Brain Res. 102, 118–128. https://doi.org/10.1016/S0169-328X(02)00216-4.

Tang, T.-S., Chen, X., Liu, J., Bezprozvanny, I., 2007. Neurobiology of Disease Dopaminergic Signaling and Striatal Neurodegeneration in Huntington's Disease. https://doi.org/10.1523/JNEUROSCI.1396-07.2007.

Tecuapetla, F., Jin, X., Lima, S.Q., Costa, R.M., 2016. Complementary contributions of striatal projection pathways to action initiation and execution. Cell 166, 703–715. https://doi.org/10.1016/j.cell.2016.06.032.

Wall, N.R., DeLaParra, M., Callaway, E.M., Kreitzer, A.C., 2013. Differential innervation of direct- and indirect-pathway striatal projection neurons. Neuron 79, 347–360. https://doi.org/10.1016/j.neuron.2013.05.014.

Yin, H.H., Mulcare, S.P., Hilário, M.R.F., Clouse, E., Holloway, T., Davis, M.I., Hansson, A.C., Lovinger, D.M., Costa, R.M., 2009. Dynamic reorganization of striatal circuits during the acquisition and consolidation of a skill. Nat. Neurosci. 12, 333–341. https://doi.org/10.1038/nn.2261.